Available online at www.sciencedirect.com

ScienceDirect

Scripta Materialia 84–85 (2014) 51–54

Scripta MATERIALIA

www.elsevier.com/locate/scriptamat

Strong crack blunting by shear-coupled migration of grain boundaries in nanocrystalline materials

Jianjun Li,[a,*] Shaohua Chen,[b] Xiaolei Wu[b] and A.K. Soh[c]

[a]*Department of Engineering Mechanics, School of Mechanics, Civil Engineering and Architecture, Northwestern Polytechnical University, Xi'an, Shanxi, China*

[b]*State Key Laboratory of Nonlinear Mechanics, Institute of Mechanics, Chinese Academy of Sciences, Beijing 100190, China*

[c]*School of Engineering, Monash University Malaysia, Bandar Sunway, Salangor, Malaysia*

Received 22 March 2014; revised 20 April 2014; accepted 22 April 2014
Available online 26 April 2014

A theoretical model is proposed to illustrate the effect of shear-coupled migration of grain boundaries on the emission of lattice dislocations from a semi-infinite crack tip in nanocrystalline materials. The results obtained show that the shear-coupled migration process is able to considerably enhance the capability of the crack to emit dislocations, thus leading to strong crack blunting. Moreover, the combination of grain boundary migration and dislocation emission can serve as an effective toughening mechanism in nanocrystalline materials.

© 2014 Acta Materialia Inc. Published by Elsevier Ltd. All rights reserved.

Keywords: Nanocrystalline materials; Shear-coupled migration of grain boundaries; Cracks; Dislocation emission; Toughening mechanism

Nanocrystalline (NC) materials are usually strong but brittle due to the suppression of the conventional dislocation slip that dominates in their coarse-grained counterparts [1]. The characteristic of low ductility has significantly limited the application of NC materials. Thus, many scientists have made great efforts in the past decades to alleviate the strength–ductility trade-off, and have successfully fabricated some strong and ductile NC materials [2–6]. Moreover, extensive recent experiments have shown that stress-driven nanograin growth plays a significant role in improving the strain hardening and ductility of NC materials [5,7–9], which provides a new way to greatly enhance the ductility of NC materials while maintaining their ultrahigh strength.

It has been shown that stress-driven nanograin growth has two main deformation modes: shear-coupled migration (SCM) of grain boundaries and nanograin rotation [10–19]. The SCM mode has been identified as a general toughening mechanism [20,21], and can considerably enhance the intrinsic ductility of NC materials [22,23]. Moreover, our recent study has shown that SCM was in favor of the dislocation emission from the disclinated grain boundaries [24]. Therefore, one may deduce that SCM could also influence the dislocation emission from a crack tip, thus leading to crack blunting and abundant activation of dislocations in the grain interior, and eventually giving rise to the enhanced ductile feature, which appeared in some NC materials as observed in experiments [3,5,7,8,25]. In this paper, we extend the model of Ovid'ko and Sheinerman [26,27] to investigate the effect of SCM on crack blunting in NC materials.

Consider a deformed elastically isotropic NC specimen, in which a long flat mode I crack is formed under an applied tensile stress σ, as shown in Figure 1a. For simplicity, a cracked two-dimensional grain structure with the crack tip located at the center of the grain boundary (GB) "AB" (Fig. 1b) is analyzed. The stresses induced by the crack are assumed to be sufficiently high to initiate a shear-coupled migration of the GB "AB" between grains G1 and G2 (Fig. 1c). The GB "AB" is assumed to migrate in a rectangular grain ABDC (i.e., G2 in Fig. 1b) over a distance m normal to GB "AB" accompanied by a tangential translation $s = \beta m$ ($\beta = \tan\varphi$) (Fig. 1c), where the coupling factor β is defined as the ratio of s to m, i.e., $\beta = s/m$ [28]. As a

* Corresponding author. Tel.: +86 13259738949; e-mail addresses: jianjunli.mech@gmail.com; mejjli@nwpu.edu.cn

http://dx.doi.org/10.1016/j.scriptamat.2014.04.020
1359-6462/© 2014 Acta Materialia Inc. Published by Elsevier Ltd. All rights reserved.

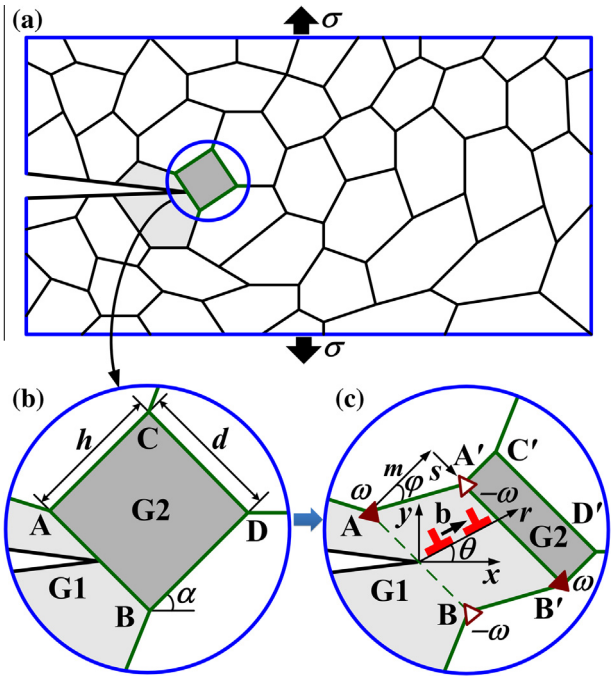

Figure 1. Lattice dislocation emission from a crack tip induced by the process of shear-coupled migration of grain boundaries in a deformed NC solid: (a) general view; (b) initial configuration of grain boundaries; and (c) configuration resulting from the dislocation emission (with Burgers vector b) after the shear-coupled migration, where "AB" is moved to $A'B'$ with an increase of size in grain G1.

result, the initial GB "AB" is moved to a new location $A'B'$. In accordance with the theory of defects in solids, the shear-coupled migration process would lead to two dipoles of wedge disclination AA' and BB' with an arm l and strength $\pm\omega$, as indicated by the triangles in Figure 1c. The two dipoles form a disclination quadruple $ABB'A'$. The shear-coupled migration of GB "AB" simultaneously gives rise to an increase and a decrease in the size of grains G1 and G2, respectively (Fig. 1c). For simplicity, the length d of "AB" can be taken as the approximate grain size of the NC specimen.

In order to consider the effect of SCM on crack blunting in a NC specimen, we assume that, accompanying the SCM of GB "AB", several edge dislocations with Burgers vector **b** are emitted from the semi-infinite crack tip along the slip plane inclining at an angle θ with respect to the x-axis, as shown in Figure 1c. According to Ovid'ko and Sheinerman [26,27], the emission criterion for the first dislocation is that the effective stress $\sigma^{e}_{r\theta}(r_1,\theta)$ at $r_1 = r_c$ (r_c is the radius of the dislocation core) should be larger than zero, i.e.,

$$\sigma^{K_I}_{r\theta}(r_1,\theta) + \sigma^{im}_{r\theta}(r_1,\theta) + \sigma^{q}_{r\theta}(r_1,\theta)\big|_{r_1=r_c} > 0 \tag{1}$$

where the stress $\sigma^{K_I}_{r\theta}(r_1,\theta)$ is produced by the applied tensile load near the crack tip, $\sigma^{im}_{r\theta}(r_1,\theta)$ depicts the image stress induced by the crack free surface and $\sigma^{q}_{r\theta}(r_1,\theta)$ is the stress induced by the disclination quadruple resulting from the shear-coupled migration of GB "AB".

The first dislocation after emission is assumed to move along the slip plane and finally stops at the new GB $A'B'$, as shown in Figure 1c. Similarly, the requirement for emission of the $(N+1)$th ($N = 1, 2, \ldots$) dislocation is:

$$\sigma^{K_I}_{r\theta}(r_{N+1},\theta) + \sigma^{im}_{r\theta}(r_{N+1},\theta) + \sigma^{q}_{r\theta}(r_{N+1},\theta) + \sum_{j=1}^{N}\sigma^{d}_{r\theta}(r_{N+1},r_j,\theta)\Big|_{r_{N+1}=r_c} > 0 \tag{2}$$

where $\sigma^{d}_{r\theta}(r_{N+1},r_j,\theta)$ is the stress exerted by the jth dislocation on the newly emitted one. For simplicity, the emitted $N+1$ dislocations are assumed to be distributed uniformly along the slip direction.

The expressions for the stresses $\sigma^{K_I}_{r\theta}(r,\theta)$ and $\sigma^{im}_{r\theta}(r,\theta)$ that appear in Eqs. (1) and (2) have been presented in Ref. [29]; these are

$$\sigma^{K_I}_{r\theta}(r,\theta) = \frac{K^{e}_{IC}\sin\theta\cos(\theta/2)}{2\sqrt{2\pi r}} \tag{3}$$

$$\sigma^{im}_{r\theta}(r,\theta) = -\frac{Gb}{4\pi(1-v)r} \tag{4}$$

where K^{e}_{IC} is the effective stress intensity factor due to the existence of the disclination quadruple and dislocations emitted from the crack tip. The expression of K^{e}_{IC} will be given later in Eq. (6). G and v are the shear modulus and Poisson's ratio, respectively, and b is the magnitude of the Burgers vector of the emitted dislocations. The shear stress $\sigma_{r\theta}(r,\theta)$, i.e., $\sigma^{q}_{r\theta}(r_{N+1},\theta)$ and $\sigma^{d}_{r\theta}(r_{N+1},r_j,\theta)$, exerts at the point (r,θ) by a disclination at point (r_j,θ_j) or a dislocation at point (r_{dj},θ) can be expressed in terms of the Cartesian stress components σ_{xx}, σ_{yy} and σ_{xy} as

$$\sigma_{r\theta} = (\sigma_{yy}-\sigma_{xx})\sin\theta\cos\theta + \sigma_{xy}\cos(2\theta) \tag{5}$$

Generally, $\sigma_{yy} = \mathrm{Re}g$, $\sigma_{xy} = -\mathrm{Im}g$, $\sigma_{xx} = \mathrm{Re}(4\Phi - g)$ and $g = \Phi + \Omega + (z-\bar{z})\bar{\Phi}'$, where Φ and Ω are two complex functions. The complex functions for the disclination quadruple and the emitted dislocations are presented in the Supplementary materials of this paper.

The effective stress intensity factor K^{e}_{IC} in Eq. (3) is introduced to account for the effect of a local plastic flow, i.e., the shear-coupled migration of GB "AB" and the slip of the dislocations emitted from the crack tip, on crack growth. By modifying a mode I brittle crack growth criterion, which is based on the balance between the energy release rate and the energy needed by a new free surface formation [21,30,31], the effective stress intensity factor can be expressed as

$$K^{e}_{IC} = \sqrt{\left(K^{\sigma}_{IC}\right)^2 - \left(k^{q}_{II}+k^{d}_{II}\right)^2} - \left(k^{q}_{I}+k^{d}_{I}\right) \tag{6}$$

where $K^{\sigma}_{IC} = \sqrt{4G\gamma_e/(1-v)}$ is the fracture toughness without considering shear-coupled migration and/or dislocation emission. k^{q}_{I} (k^{q}_{II}) and k^{d}_{I} (k^{d}_{II}) are the stress intensity factors generated by the disclination quadruple $BB'A'A$ and the emitted dislocations located near the crack, respectively (Fig. 1c), which can be obtained from the following definition [29]:

$$k^{r}_{I} + ik^{r}_{II} = \lim_{z\to 0} 2\sqrt{2\pi z}\,\Phi^{r}(z) \tag{7}$$

where the superscript "r" represents either "q" or "d", which indicate either disclination quadruple or

dislocations emitted from the crack tip, respectively. Combining Eqs. (S1) and (7), we obtain

$$k_{\mathrm{I}}^{\mathrm{q}}=\frac{G\omega}{2\sqrt{2\pi}(1-\nu)}\sum_{j=1}^{4}(-1)^{j}\sqrt{r_j}\left(3\cos\frac{\theta_j}{2}+\cos\frac{3\theta_j}{2}\right)$$

$$k_{\mathrm{II}}^{\mathrm{q}}=\frac{G\omega}{2\sqrt{2\pi}(1-\nu)}\sum_{j=1}^{4}(-1)^{j}\sqrt{r_j}\left(\sin\frac{\theta_j}{2}+\sin\frac{3\theta_j}{2}\right) \quad (8)$$

where r_j, θ_j are coordinates of the jth disclination (see Supplementary materials for their expressions); $j=1$, 2, 3, 4 corresponds to disclination B, B', A' and A, respectively, as shown in Figure 1c; and $\theta_j \in (-\pi, \pi)$. Similarly, by combining Eqs. (S3) and (7), we obtain

$$k_{\mathrm{I}}^{\mathrm{d}}=\frac{Gb}{2\sqrt{2\pi}(1-\nu)}\sum_{j=1}^{N}\frac{(-1)^{j}}{\sqrt{r_{dj}}}\left(-\frac{3}{2}\sin\frac{\theta}{2}-\frac{3}{2}\sin\frac{3\theta}{2}\right)$$

$$k_{\mathrm{II}}^{\mathrm{d}}=\frac{Gb}{2\sqrt{2\pi}(1-\nu)}\sum_{j=1}^{N}\frac{(-1)^{j}}{\sqrt{r_{dj}}}\left(\frac{1}{2}\cos\frac{\theta}{2}+\frac{3}{2}\cos\frac{3\theta}{2}\right) \quad (9)$$

where N is the number of emitted dislocations and $(r_{dj}, \theta$ is the position of the jth emitted dislocation.

In order to find the maximum number of dislocations $N_{\max}$, we adopt the following procedure: (i) Eq. (1) is used to verify the emission possibility of the first dislocation; (ii) if Eq. (1) is satisfied, Eq. (2) is then employed to check the possibility of emission of the second dislocation; (iii) repeat step (ii) for the subsequent impending dislocations. The following parametric values of NC Ni are adopted in the present calculation: $G=73$ GPa, $\nu=0.34$, $\gamma=1.725$ J/m^2, $b=0.25$ nm, $r_c=2b$, $\omega=0.3$, $\theta=\pi/6$, $\alpha=\pi/3$.

The variation of the maximum number of dislocations $N_{\max}$ emitted from the crack tip with the grain size d for various coupling factors ($\beta=0$, 1, 3) and normal migration distances ($m=5$ nm, 8 nm) are presented in Figure 2, in which the results for a brittle NC Ni without considering the SCM process are also included for comparison. Figure 2 shows that $N_{\max}$ for brittle Ni (without SCM) increases monotonously from 2 to 4 as the grain size d is increased from 5 nm to 100 nm, which is in good

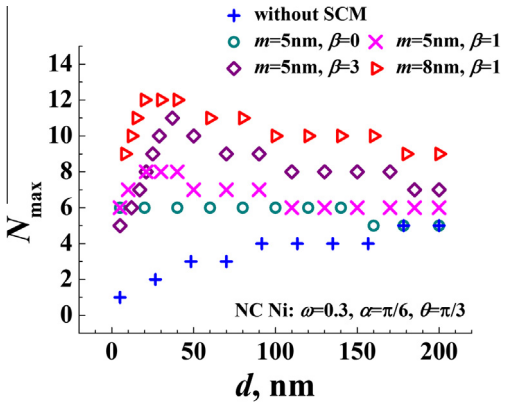

Figure 2. Variation of the maximum number of edge dislocations $N_{\max}$ with respect to the grain size d in the case where SCM is a dominating deformation mode. Various values of migration distance m and coupling factor β are considered; moreover, the case of brittle Ni (without SCM) is also presented for comparison.

consistency with the results obtained by Ovid'ko and Sheinerman [26]. Such low values of $N_{\max}$ lead to a brittle behavior as commonly observed in NC materials. In contrast, for a NC Ni with SCM dominating the deformation mode, $N_{\max}$ first increases to a maximum and then decreases with increasing grain size. The largest value of $N_{\max}$ corresponds to a critical grain size of 20–30 nm for all the parametric values considered. Most importantly, the value of $N_{\max}$ in a NC Ni with SCM dominating is much higher than that of the NC Ni with SCM completely suppressed. Specifically, in the case of $m=5$ nm, the largest value of $N_{\max}$ increases from 6 to 11 as β is increased from 0 to 3. These β values are easily accessible in the recent experimental and theoretical analyses [32,33]. The value of $N_{\max}$ can be further improved from 8 to 12 by increasing m from 5 nm to 8 nm. Such a considerable enhancement by a maximum factor of 6 for the maximum number of dislocations emitted from the crack tip under the SCM mechanism is very conducive for induction of a strong crack blunting in NC materials. Thus, the original brittle NC solids become ductile due to the presence of SCM.

The occurrence of the critical grain size at ~20–30 nm in the case where SCM is dominating are attributed to SCM since no such behavior was observed in the case without SCM. As a matter of fact, examination of the effective stress created by SCM, i.e., $\sigma_{r\theta}^{q}(r_{N+1},\theta)$ as appearing in Eqs. (1) and (2), enables us to find out that it exhibits a first-increase-and-then-decrease trend with increasing grain size. This trend undoubtedly determined the trend of variation of $N_{\max}$ with respect to d in the case where SCM is the dominating deformation mode. On the other hand, nanograined metals/alloys are usually strong but become increasingly brittle due to the increasing difficulty of the conventional dislocation slip that is prevalent in their coarse-grained counterparts, especially as the grain size is refined below ~20–50 nm [1]. In such small grain size scale, the conventional dislocation slip gives way to GB-mediated deformation modes such as GB sliding [34], grain rotation [35] and SCM [36]. At the same time, it becomes much more difficult for dislocations to pile up at a GB in an extremely small grain of size less than 10–20 nm, even though SCM can enhance dislocation emission. Therefore, it is conceivable that SCM plays a maximum role at grains of ~20–30 nm in improving the capacity of a crack tip to emit dislocations which would pile up at a migrated GB. The revealing of the critical grain size and the corresponding high value of $N_{\max}$ explain why SCM becomes increasingly dominating in some ductile nanograined metals and their composite counterparts with an average grain size of ~20–30 nm, as observed in some experiments (e.g., Refs. [3,5,7]).

To date, the effective toughening mechanism in NC materials, SCM, has been well studied [21]. A natural further study is to consider the combined effect of SCM and the emitted dislocations promoted by SCM on the fracture toughness of NC materials, which is represented by an effective stress intensity factor $K_{\mathrm{IC}}^{\mathrm{e}}$, as given in Eq. (6). An improved toughening behavior is achieved if $K_{\mathrm{IC}}^{\mathrm{e}}/K_{\mathrm{IC}}^{\sigma} \geqslant 1$. The grain size dependent effective stress intensity for a NC Ni at $\beta=1$ and $m=5$ is presented in Figure 3, where the case without considering

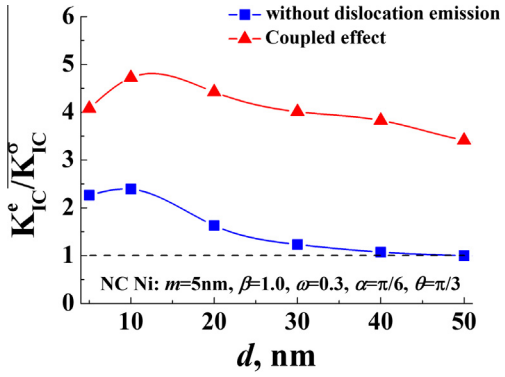

Figure 3. Variation of normalized effective stress intensity factor K^e_{IC}/K^σ_{IC} obtained from a NC Ni subjected to the coupling effect of shear-coupled migration and dislocation emission with grain size. The results obtained for the corresponding materials with only shear-coupled migration considered are also presented for comparison.

dislocation emission is also presented for comparison. Figure 3 clearly shows that all the values of K^e_{IC}/K^σ_{IC} are larger than 1 for grain size d lying in the range of 0–50 nm, and the maximum K^e_{IC}/K^σ_{IC} of ~4.72 occurs at a critical grain size of ~10 nm. Such a value of K^e_{IC}/K^σ_{IC} is approximately two times that of a NC Ni without considering dislocation emission. One may infer from the above results that emission of dislocations from a crack tip accompanied by SCM is very effective for toughening NC materials.

In summary, a theoretical model has been developed to investigate the effect of shear-coupled migration of grain boundaries on crack blunting in NC materials. The results obtained show that the migration process can greatly enhance the maximum number of dislocations emitted from a semi-crack tip, which facilitates a strong crack blunting and thus improves the ductility of the originally brittle NC materials. Moreover, the combined effect of SCM and emission of induced dislocations can significantly increase the effective stress intensity factor, which leads to a new effective toughening mechanism in NC materials. The proposed model provides a possible explanation for the high ductility as well as strong strain hardening behavior observed in some NC samples studied recently [3,5,7,8].

J.L. acknowledges the financial support by the Start-up funding (No. 13GH0316) for the Newly-recruited High-level Talents from Northwestern Polytechnical University, China. S.C. thanks the support from NSFC through Grants #11125211, #11372317 and the 973 Nano-project (2012CB937500). A.K.S. acknowledges the support of the Advanced Engineering Programme and School of Engineering, Monash University Malaysia, as well as the eScience grant (Project No.: 06-02-10-SF0195) provided by the Ministry of Science, Technology and Innovation (MOSTI), Malaysia.

Supplementary data associated with this article can be found, in the online version, at http://dx.doi.org/10.1016/j.scriptamat.2014.04.020.

[1] M.A. Meyers, A. Mishra, D.J. Benson, Prog. Mater Sci. 51 (2006) 427–556.
[2] K.M. Youssef, R.O. Scattergood, K.L. Murty, J.A. Horton, C.C. Koch, Appl. Phys. Lett. 87 (2005) 091904.
[3] S. Cheng, Y. Zhao, Y. Guo, Y. Li, Q. Wei, X.L. Wang, Y. Ren, P.K. Liaw, H. Choo, E.J. Lavernia, Adv. Mater. 21 (2009) 5001–5004.
[4] L. Lu, X. Chen, X. Huang, K. Lu, Science 323 (2009) 607–610.
[5] T.H. Fang, W.L. Li, N.R. Tao, K. Lu, Science 331 (2011) 1587–1590.
[6] Y.M. Wang, R.T. Ott, A.V. Hamza, M.F. Besser, J. Almer, M.J. Kramer, Phys. Rev. Lett. 105 (2010) 215502.
[7] D.S. Gianola, S. Van Petegem, M. Legros, S. Brandstetter, H. Van Swygenhoven, K.J. Hemker, Acta Mater. 54 (2006) 2253–2263.
[8] X. Wu, Y. Zhu, Y. Wei, Q. Wei, Phys. Rev. Lett. 103 (2009) 205504.
[9] G.J. Fan, L.F. Fu, H. Choo, P.K. Liaw, N.D. Browning, Acta Mater. 54 (2006) 4781–4792.
[10] M. Jin, A.M. Minor, E.A. Stach, J.W. Morris, Acta Mater. 52 (2004) 5381–5387.
[11] J. Monk, D. Farkas, Phys. Rev. B 75 (2007) 045414.
[12] W.A. Soer, J.T.M. De Hosson, A.M. Minor, J.W. Morris, E.A. Stach, Acta Mater. 52 (2004) 5783–5790.
[13] A. Haslam, D. Moldovan, V. Yamakov, D. Wolf, S. Phillpot, H. Gleiter, Acta Mater. 51 (2003) 2097–2112.
[14] K. Zhang, J.R. Weertman, J.A. Eastman, Appl. Phys. Lett. 87 (2005) 061921.
[15] T. Gorkaya, T. Burlet, D.A. Molodov, G. Gottstein, Scripta Mater. 63 (2010) 633–636.
[16] M. Winning, A. Rollett, G. Gottstein, D. Srolovitz, A. Lim, L. Shvindlerman, Philos. Mag. 90 (2010) 3107–3128.
[17] M.Y. Gutkin, I.A. Ovid'ko, Appl. Phys. Lett. 87 (2005) 251916.
[18] J. Li, A.K. Soh, X. Wu, Scripta Mater. 78–79 (2014) 5–8.
[19] J. Li, S. Chen, Mater. Lett. 121 (2014) 174–176.
[20] J. Li, A.K. Soh, Appl. Phys. Lett. 101 (2012) 241915.
[21] J. Li, A.K. Soh, Scripta Mater. 69 (2013) 283–286.
[22] J. Li, A.K. Soh, Acta Mater. 61 (2013) 5449–5457.
[23] I.A. Ovid'ko, A.G. Sheinerman, E.C. Alfantis, Acta Mater. 56 (2008) 2718–2727.
[24] J. Li, A.K. Soh, X. Wu, Mat. Sci. Eng. A 601 (2014) 153–158.
[25] X.L. Wu, E. Ma, Appl. Phys. Lett. 88 (2006) 231911.
[26] I.A. Ovid'ko, A.G. Sheinerman, Scripta Mater. 60 (2009) 627–630.
[27] I. Ovid'ko, A. Sheinerman, Acta Mater. 58 (2010) 5286–5294.
[28] J.W. Cahn, Y. Mishin, A. Suzuki, Acta Mater. 54 (2006) 4953–4975.
[29] I.-H. Lin, R. Thomson, Acta Metall. 34 (1986) 187–206.
[30] G. Irwin, J. Appl. Mech. 24 (1957) 361–364.
[31] N.F. Morozov, I.A. Ovid'ko, A.G. Sheinerman, E.C. Aifantis, J. Mech. Phys. Solids 58 (2010) 1088–1099.
[32] D. Caillard, F. Mompiou, M. Legros, Acta Mater. 57 (2009) 2390–2402.
[33] F. Mompiou, D. Caillard, M. Legros, Acta Mater. 57 (2009) 2198–2209.
[34] J. Schiotz, K.W. Jacobsen, Science 301 (2003) 1357–1359.
[35] Z.W. Shan, E.A. Stach, J.M.K. Wiezorek, J.A. Knapp, D.M. Follstaedt, S.X. Mao, Science 305 (2004) 654–657.
[36] D. Farkas, A. Froseth, H. Van Swygenhoven, Scripta Mater. 55 (2006) 695–698.